

Conduction and valence band offsets of LaAl_2O_3 with (-201) $\beta\text{-Ga}_2\text{O}_3$

Patrick H. Carey, Fan Ren, David C. Hays, Brent P. Gila, Stephen J. Pearton, Soohwan Jang, and Akito Kuramata

Citation: *Journal of Vacuum Science & Technology B* **35**, 041201 (2017); doi: 10.1116/1.4984097

View online: <https://doi.org/10.1116/1.4984097>

View Table of Contents: <http://avs.scitation.org/toc/jvb/35/4>

Published by the [American Vacuum Society](#)

Articles you may be interested in

[Inductively coupled plasma etching of bulk, single-crystal \$\text{Ga}_2\text{O}_3\$](#)

Journal of Vacuum Science & Technology B, Nanotechnology and Microelectronics: Materials, Processing, Measurement, and Phenomena **35**, 031205 (2017); 10.1116/1.4982714

[Inductively coupled plasma reactive-ion etching of \$\beta\text{-Ga}_2\text{O}_3\$: Comprehensive investigation of plasma chemistry and temperature](#)

Journal of Vacuum Science & Technology A: Vacuum, Surfaces, and Films **35**, 041301 (2017); 10.1116/1.4983078

[\$\beta\text{-\(Al}_x\text{Ga}_{1-x}\)_2\text{O}_3/\text{Ga}_2\text{O}_3\$ \(010\) heterostructures grown on \$\beta\text{-Ga}_2\text{O}_3\$ \(010\) substrates by plasma-assisted molecular beam epitaxy](#)

Journal of Vacuum Science & Technology A: Vacuum, Surfaces, and Films **33**, 041508 (2015); 10.1116/1.4922340

[Schottky barrier diode based on \$\beta\text{-Ga}_2\text{O}_3\$ \(100\) single crystal substrate and its temperature-dependent electrical characteristics](#)


Applied Physics Letters **110**, 093503 (2017); 10.1063/1.4977766

[Structural and optical properties of \$\beta\text{-Ga}_2\text{O}_3\$ thin films grown by plasma-assisted molecular beam epitaxy](#)

Journal of Vacuum Science & Technology B, Nanotechnology and Microelectronics: Materials, Processing, Measurement, and Phenomena **34**, 02L109 (2016); 10.1116/1.4942045

[Effects of post-annealing temperature and oxygen concentration during sputtering on the structural and optical properties of \$\beta\text{-Ga}_2\text{O}_3\$ films](#)

Journal of Vacuum Science & Technology A: Vacuum, Surfaces, and Films **34**, 060602 (2016); 10.1116/1.4963376



Instruments for Advanced Science

Contact Hiden Analytical for further details:
W www.HidenAnalytical.com
E info@hiden.co.uk

CLICK TO VIEW our product catalogue

Gas Analysis	Surface Science	Plasma Diagnostics	Vacuum Analysis
 <ul style="list-style-type: none">dynamic measurement of reaction gas streamscatalysis and thermal analysismolecular beam studiesdissolved species probesfermentation, environmental and ecological studies	 <ul style="list-style-type: none">UHV TPDSIMSend point detection in ion beam etchelemental imaging - surface mapping	 <ul style="list-style-type: none">plasma source characterizationetch and deposition process reaction kinetic studiesanalysis of neutral and radical species	 <ul style="list-style-type: none">partial pressure measurement and control of process gasesreactive sputter process controlvacuum diagnosticsvacuum coating process monitoring

Conduction and valence band offsets of LaAl_2O_3 with (-201) $\beta\text{-Ga}_2\text{O}_3$

Patrick H. Carey IV and Fan Ren

Department of Chemical Engineering, University of Florida, Gainesville, Florida 32611

David C. Hays, Brent P. Gila, and Stephen J. Pearton^{a)}

Department of Materials Science and Engineering, University of Florida, Gainesville, Florida 32611

SooHwan Jang

Department of Chemical Engineering, Dankook University, Yongin 16890, South Korea

Akito Kuramata

Tamura Corporation, Sayama, Saitama 350-1328, Japan and Novel Crystal Technology, Inc., Sayama, Saitama 350-1328, Japan

(Received 13 April 2017; accepted 11 May 2017; published 24 May 2017)

Wide bandgap dielectrics are needed as gate insulators and surface passivation layers on the emerging electronic oxide Ga_2O_3 . X-ray photoelectron spectroscopy was used to determine the valence band offset at LaAl_2O_3 (LAO)/ $\beta\text{-Ga}_2\text{O}_3$ heterointerfaces. LaAl_2O_3 was deposited by RF magnetron sputtering onto bulk Ga_2O_3 crystals. The bandgaps of the materials were determined by reflection electron energy loss spectroscopy to be 4.6 eV for Ga_2O_3 and 6.4 eV for LAO. The valence band offset was determined to be -0.21 ± 0.02 eV (staggered gap, type II alignment) for LAO on Ga_2O_3 . This leads to a conduction band offset of 2.01 ± 0.60 eV for LAO with Ga_2O_3 . Thus, LAO provides excellent electron confinement but not hole confinement in LAO/ Ga_2O_3 heterostructures. © 2017 American Vacuum Society. [<http://dx.doi.org/10.1116/1.4984097>]

I. INTRODUCTION

The β -polytype of Ga_2O_3 is a candidate for both high voltage electronics and truly solar-blind UV photodetectors.^{1–13} It has a number of attractive features, including a larger bandgap than either GaN or SiC and availability in a large diameter, high quality single-crystal form.^{1–3} The large bandgap means that it is capable of achieving high reverse breakdown voltages in rectifier and transistor structures, with values over 1kV already reported for vertical diodes.¹⁴ This material is a readily doped n-type over a wide range of conductivities, and there are recent reports of high quality epi films on bulk substrates.^{1–4} There is a need to develop a robust metal-oxide-semiconductor field effect transistor technology for Ga_2O_3 ^{8,9,11,12} as well as have surface passivation films that are easily deposited and are selectively patternable relative to Ga_2O_3 .^{4,11,15} Given the wide bandgap of Ga_2O_3 , there are a relatively limited number of candidate gate dielectrics for these applications, including Al_2O_3 , HfO_2 , and SiO_2 .^{16–19} These have typically been deposited by atomic layer deposited (ALD) or plasma enhanced chemical vapor deposition. For gate dielectrics, it is desirable that both conduction and valence band offsets (VBOs) are ≥ 1 eV to achieve strong electron and hole confinement in heterostructures.^{20–22}

LaAlO_3 (LAO) deposited by physical vapor deposition typically has a bandgap of around 6.5 eV and a dielectric constant of ~ 22 and is a potential candidate for use with Ga_2O_3 given its large bandgap.²³ LAO was extensively investigated as a high-k dielectric for Si but did not have a sufficiently stable interface with Si at the necessary processing temperatures.²³

In this paper, we report on the determination of the band alignment in the LAO/ Ga_2O_3 heterostructure, in which LAO

was deposited by sputtering. We employ x-ray photoelectron spectroscopy (XPS)^{24,25} to determine the valence band offsets, and by measuring the respective bandgaps of LAO (6.4 eV) and Ga_2O_3 (4.6 eV), we were also able to determine the conduction band offset in LAO/ Ga_2O_3 heterostructures. The band alignment is found to be of type II.

II. EXPERIMENT

LAO was deposited by RF magnetron sputtering on Ga_2O_3 and quartz substrates. The sputtering was carried out at room temperature using a 3-in. diameter target of pure LAO. The RF power was 355 W, and the deposition pressure was 5 mTorr in a pure Ar ambient. The bulk β -phase Ga_2O_3 single crystals with (-201) surface orientation (Tamura Corporation, Japan) were grown by the edge-defined film-fed growth method. Hall effect measurements showed that the sample was unintentionally n-type with an electron concentration of $\sim 3 \times 10^{17} \text{ cm}^{-3}$. The samples were not exposed to air prior to the subsequent XPS measurements to avoid complications from surface contamination. The latter may lead to less accurate band gap measurements when using reflection electron energy loss spectroscopy (REELS).

The method described in the study by Kraut *et al.*^{24,25} using x-ray photoemission spectroscopy has been established as a reliable way to determine band offsets at the heterojunction interface. It is based on using an appropriate shallow core-level position as a reference. Generally, this approach is based on the assumption that the energy difference between the core-level positions and the valence-band maximum (VBM) is fixed in the bulk.²⁶ The basic method is to first measure the energy difference between a core level and the VBM for both the single layer dielectric and the semiconductor. One measures the reference core level binding

^{a)}Electronic mail: spear@mse.ufl.edu

energies in thick films of each material and then measures the binding energy difference between the two reference core levels in the heterojunction. The value of ΔE_V is determined by combining those three quantities.

Heterojunction samples, consisting of a thin (1.5 nm) layer of LAO deposited on Ga_2O_3 , were prepared, and the separation between reference core levels in each material was measured. The separation between the reference core levels was then translated directly into a value for the VBO using the previously measured single layer sample core-level to VBM energies. To measure the valence band offsets, XPS survey scans were performed to determine the chemical state of LAO and Ga_2O_3 and identify peaks for high resolution analysis.^{24,25} A Physical Electronics PHI 5100 XPS with an aluminum x-ray source (energy 1486.6 eV) with a source power of 300 W was used, with an analysis area of 2×0.8 mm, a take-off angle of 50° , and an acceptance angle of $\pm 7^\circ$. The electron pass energies were 23.5 eV for the high resolution scans and 187.5 eV for the survey scans. The approximate escape depth ($3\lambda \sin \theta$) of the electrons was 80 Å. All the peaks were well-defined in this system, and we did not need to curve fit the data.

Charge compensation was performed using an electron flood gun.²⁶ The charge compensation flood gun is often not efficient in eliminating all surface charge, and additional corrections must be performed. Using the known position of the adventitious carbon (C-C) line in the C 1s spectra at 284.8 eV, charge correction was performed. During the measurements, all the samples and electron analyzers were electrically grounded, providing a common reference Fermi level. Differential charging is a serious concern for photoemission dielectric/semiconductor band offset measurements.²⁶ While the use of an electron flood gun does not guarantee that differential charging is not present and in some cases could make the problem worse, our experience with oxides on conducting substrates has been that the differential charging is minimized with the use of an electron gun. Calibrations performed with and without the electron gun operating showed this was the case.

REELS was employed to measure the bandgaps of LAO and Ga_2O_3 .²⁷⁻³¹ REELS spectra were obtained using a 1 kV electron beam and a hemispherical electron analyzer.

III. RESULTS AND DISCUSSION

Figure 1 shows the stacked XPS survey scans of thick (200 nm) sputtered deposited LAO, 1.5 nm sputtered LAO on Ga_2O_3 , and the bulk Ga_2O_3 crystal. The spectra are free from contaminants and consistent with previously published XPS data.^{22,23,32} In particular, we looked carefully for the presence of metallic contaminants in the sputtered films whose oxides might lower the overall bandgap of LAO and thus affect the band alignment.³³⁻³⁷ However, these were not detected to the sensitivity level of XPS.

The valence band maximum (VBM) was determined by linearly fitting the leading edge of the valence band and the flat energy distribution from the XPS measurements and finding the intersection of these two lines,^{25,26} as shown in

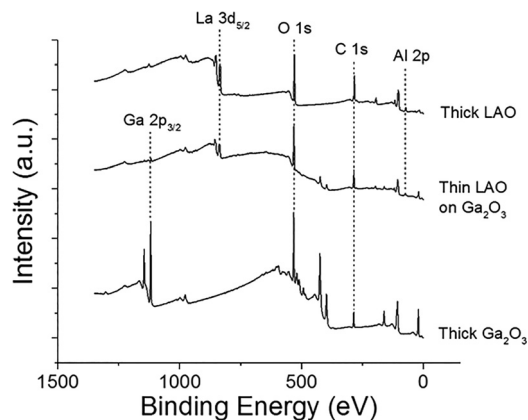


Fig. 1. XPS survey scans of thick sputtered LaAlO_3 , 1.5 nm sputtered LaAlO_3 on Ga_2O_3 , and Ga_2O_3 bulk samples.

Fig. 2 for the bulk Ga_2O_3 (a) and thick LAO (b). The VBM was measured to be 3.2 ± 0.2 eV for Ga_2O_3 , which is consistent with previous reports,³² and 2.3 ± 0.2 eV for the sputtered LAO, which is also similar to previous measurements.²³

The bandgap of Ga_2O_3 was determined to be 4.6 ± 0.3 eV, as shown in the REELS spectra in Fig. 3(a). The band gap was determined from the onset of the energy loss spectrum.^{26,30} The bandgap of Ga_2O_3 is a function of the polytype, and it is common in the literature to quote a value of ~ 4.8 eV for $\beta\text{-Ga}_2\text{O}_3$, but we and others have noted that optical

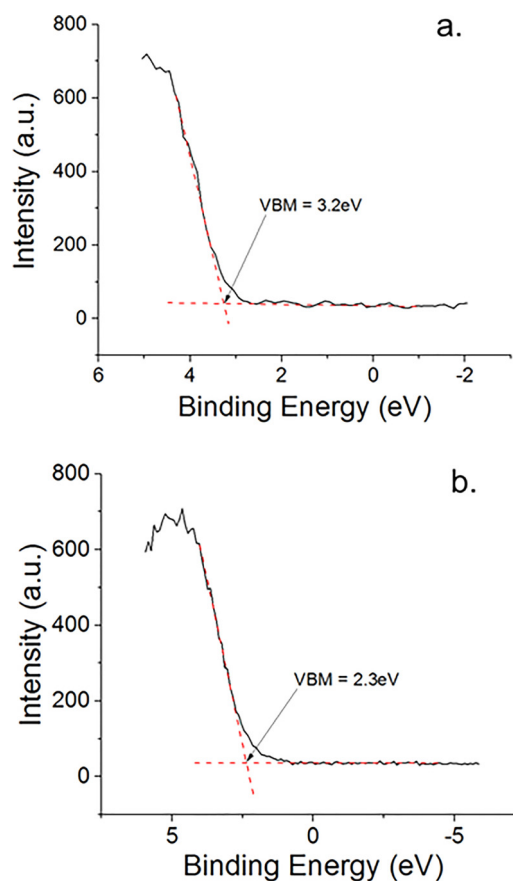


Fig. 2. (Color online) XPS spectra of core levels to the valence band maximum (VBM) for (a) bulk Ga_2O_3 and (b) thick film LaAlO_3 .

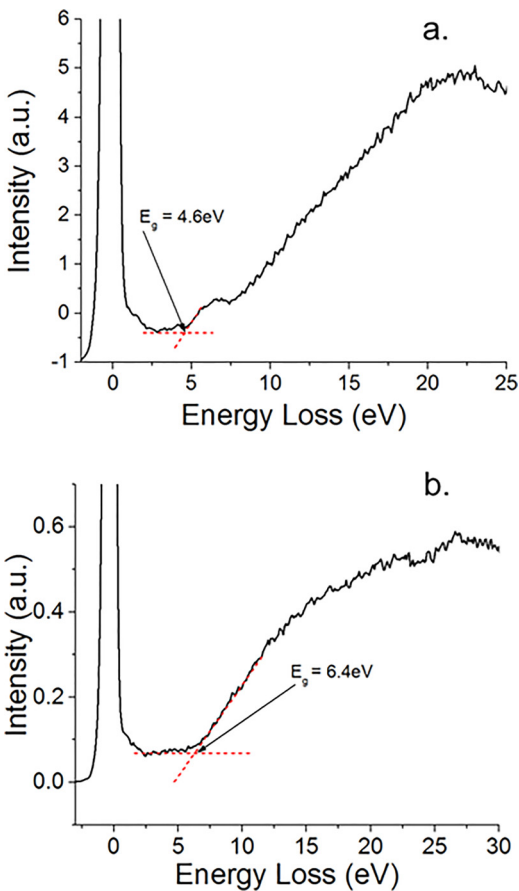


Fig. 3. (Color online) Reflection electron energy loss spectra to determine the bandgap of (a) bulk Ga_2O_3 (top) and (b) thick LaAlO_3 .

transmittance and REELS data show a consistent value of 4.6 eV.^{17,32,38} He *et al.*³⁹ reported a direct gap of 4.69 eV, Varley calculated an indirect gap of 4.83 eV,⁴⁰ while Peelaers *et al.*⁴¹ reported an indirect gap of 4.84 eV. It seems clear that due to the often phase-impure nature of early Ga_2O_3 samples and the small energy difference between direct and indirect gaps,⁴² there can be experimental uncertainties in establishing the bandgap. In REELS, the onset of single particle excitations can be observed as a step at an energy equal to the band gap E_g below the core level and the band-gap found by drawing a linear fit line with the maximum negative slope from a point near the onset of the loss signal spectrum to the background level, as shown in Fig. 3(a). The energy corresponding to the onset of inelastic losses is found by extrapolating the linear-fit line and calculating its intersection with the “zero” level.⁴³ The band gap is the difference between the centroid of elastic scattering and the calculated intersection. The precision of finding the band gap is limited because the slope of the loss feature may not be very different from that of the background of the XPS spectrum, making background subtraction difficult. One issue we have noticed in measuring bandgaps of dielectrics using REELS is the effect of contamination from carbon and water, as well as defects.⁴³ These can lead to high backgrounds in the spectrum, can create a higher energy shoulder, or can “smear” the energy distribution. The onset of energy loss then becomes difficult to distinguish; a

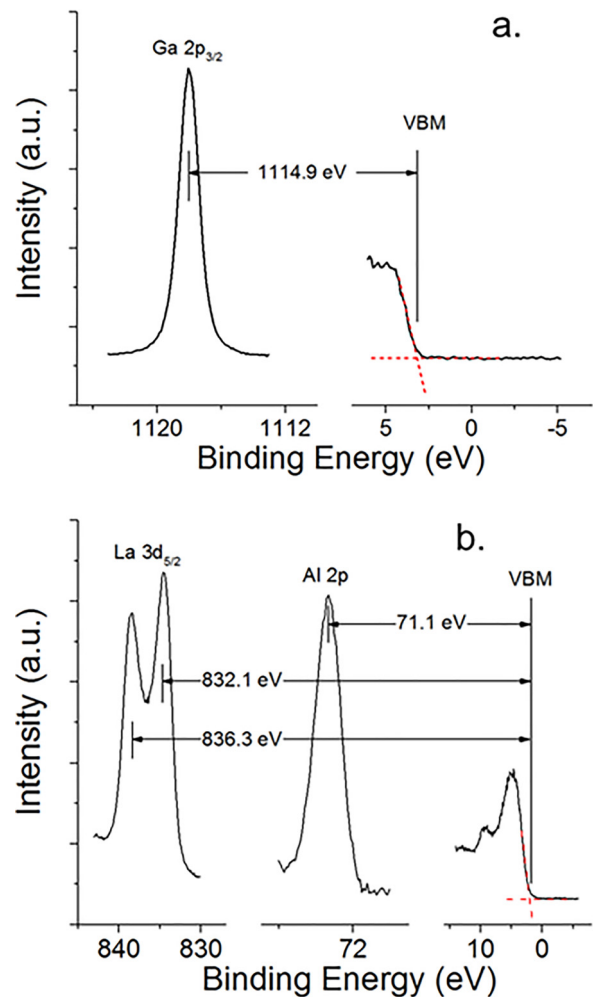


Fig. 4. (Color online) High resolution XPS spectra of the vacuum-core delta regions of (a) bulk Ga_2O_3 and (b) LaAlO_3 .

traditional fit to a horizontal line may give lower values, and fitting to a lower slope can give artificially higher values of the bandgap. The measured band gap for the sputtered LAO was found to be 6.4 ± 0.6 eV from the REELS data shown in Fig. 3(b), which is consistent with literature values.²³ The difference in bandgaps between Al_2O_3 and Ga_2O_3 is therefore 1.8 eV. To determine the actual band alignment and the

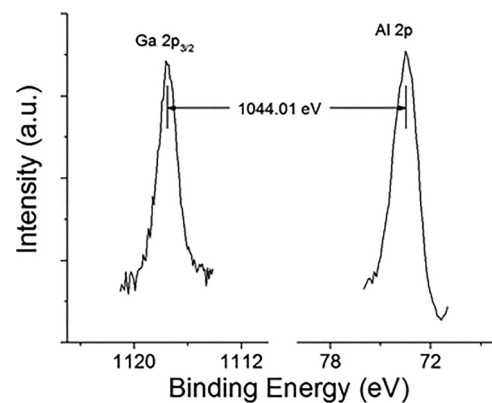


Fig. 5. High resolution XPS spectra for the Ga_2O_3 to LaAlO_3 -core delta regions.

TABLE I. Values of band offsets determined in these experiments (eV).

Reference Ga ₂ O ₃				Reference LaAlO ₃			LaAlO ₃ on Ga ₂ O ₃	
Ga ₂ O ₃ metal core	Ga ₂ O ₃ VBM	Core level	Metal core–VBM	LaAlO ₃ VBM	Al 2p core level	Al 2p–VBM	ΔCL Ga 2p _{3/2} –Al 2p	Valence band offset
Ga2p _{3/2}	3.20	1118.10	1114.90	2.30	73.40	71.10	1044.01	–0.21

respective valence and conduction band offsets, we examined the core level spectra of the samples.

High resolution XPS spectra of the VBM-core delta region are shown in Fig. 4 for the Ga₂O₃ (a) and thick sputtered LAO (b) samples. These data were then used to determine the core level peak positions. Figure 5 shows the XPS spectra for the Ga₂O₃ to LAO-core delta regions of the heterostructure samples. These values are summarized in Table I and were substituted into the following equation to calculate ΔE_V:^{24–26}

$$\Delta E_V = (E_{Core} - E_{VBM})_{Ref.Ga_2O_3} - (E_{Core} - E_{VBM})_{Ref.LAO} - (E_{Core}^{Ga_2O_3} - E_{Core}^{LAO})_{LAO/Ga_2O_3}$$

Figure 6 shows the simplified and detailed band diagrams of the LAO/Ga₂O₃ heterostructure. Our data show that the alignment is a staggered, type II alignment with a valence band offset of –0.21 ± 0.05 eV and the conduction band offset is then 2.01 ± 0.5 eV using the following equation: ΔE_C = E_g^{LAO} – E_g^{Ga₂O₃} – ΔE_V,

$$\text{i.e., } \Delta E_C = 6.4 \text{ eV} - 4.6 \text{ eV} - (-0.21 \text{ eV}) = 2.01 \text{ eV}.$$

This result shows that LAO used as a gate dielectric on Ga₂O₃ would provide excellent electron confinement but no

barrier to hole transport. It might also be used as a surface passivation layer to prevent surface conductivity changes upon exposure to ambient. The sensitivity of Ga₂O₃ to water vapor and hydrogen is not yet firmly established, but many oxides like ZnO and InGaZnO₄ do show such sensitivity and require surface passivation to provide device stability in humid ambient.

It appears that both Al₂O₃, with conduction and valence band offsets of 1.5 and 0.7 eV,¹⁸ respectively, and SiO₂, with a conduction band offset of 3.1 and a valence band offset of 1.0 eV,¹⁷ are superior choices as gate dielectrics on Ga₂O₃. Wheeler *et al.*¹⁹ measured the band alignment between ALD ZrO₂ or HfO₂ and β-Ga₂O₃, and both dielectrics resulted in a type II, staggered gap alignment with conduction band offsets of 1.2 and 1.3 eV for ZrO₂ and HfO₂ films. Our data for LAO fall into the latter category.

IV. SUMMARY AND CONCLUSIONS

The alignment at LaAlO₃/Ga₂O₃ heterojunctions is found to be a staggered gap alignment of band offsets with a valence band offset of –0.21 eV and a conduction band offset of 2.01 eV determined from XPS measurements. The conduction band offset is large enough to provide excellent electron confinement, but there is no barrier to hole transport. LAO could still be an option as a surface passivation layer on Ga₂O₃.

$$\Delta E_C = E_g^{LaAlO_3} - E_g^{Ga_2O_3} - \Delta E_V \quad \Delta E_C = 6.4 \text{ eV} - 4.6 \text{ eV} - (-0.21 \text{ eV}) = 2.01 \text{ eV}$$

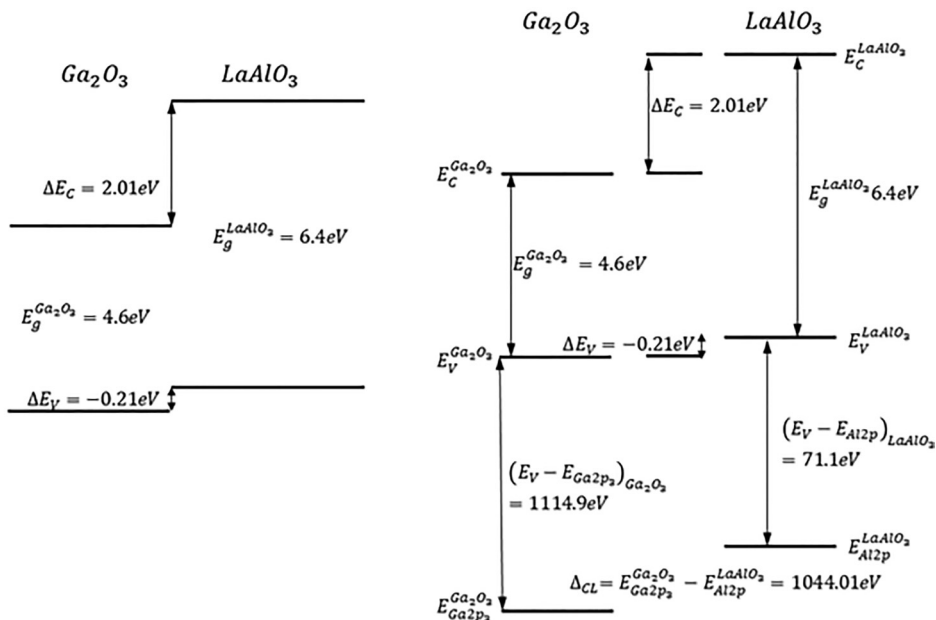


FIG. 6. Simple and detailed and diagrams of LaAlO₃/Ga₂O₃ heterostructures.

ACKNOWLEDGMENTS

The project or effort presented was also sponsored by the Department of the Defense, Defense Threat Reduction Agency, HDTRA1-17-1-011, monitored by Jacob Calkins. The content of the information does not necessarily reflect the position or the policy of the federal government, and no official endorsement should be inferred. The research at Dankook was supported by the Basic Science Research Program through the National Research Foundation of Korea (NRF) funded by the Ministry of Education (2014R1A1A4A01008877, 2015R1D1A1A01058663) and Nano Material Technology Development Program through the National Research Foundation of Korea (NRF) funded by the Ministry of Science, ICT and Future Planning (2015M3A7B7045185). Part of the work at Tamura was supported by “The research and development project for innovation technique of energy conservation” of the New Energy and Industrial Technology Development Organization (NEDO), Japan. The authors also thank Kohei Sasaki from Tamura Corporation for fruitful discussions.

- ¹A. Kuramata, K. Koshi, S. Watanabe, Y. Yamaoka, T. Masui, and S. Yamakoshi, *Jpn. J. Appl. Phys., Part 1* **55**, 1202A2 (2016).
- ²Z. Galazka *et al.*, *ECS J. Solid State Sci. Technol.* **6**, Q3007 (2017).
- ³M. Baldinuz, M. Albrecht, A. Fiedler, K. Irmscher, R. Schewski, and G. Wagner, *ECS J. Solid State Sci. Technol.* **6**, Q3040 (2017).
- ⁴M. Higashiwaki, K. Sasaki, H. Murakami, Y. Kumagai, A. Koukitu, A. Kuramata, T. Masui, and S. Yamakoshi, *Semicond. Sci. Technol.* **31**, 034001 (2016).
- ⁵A. M. Armstrong, M. H. Crawford, A. Jayawardena, A. Ahyi, and S. Dhar, *J. Appl. Phys.* **119**, 103102 (2016).
- ⁶M. Higashiwaki, K. Sasaki, A. Kuramata, T. Masui, and S. Yamakoshi, *Phys. Status Solidi A* **211**, 21 (2014).
- ⁷K. D. Chabak *et al.*, *Appl. Phys. Lett.* **109**, 213501 (2016).
- ⁸A. J. Green *et al.*, *IEEE Electron Device Lett.* **37**, 902 (2016).
- ⁹M. H. Wong, K. Sasaki, A. Kuramata, S. Yamakoshi, and M. Higashiwaki, *IEEE Electron Device Lett.* **37**, 212 (2016).
- ¹⁰S. Oh, G. Yang, and J. Kim, *ECS J. Solid State Sci. Technol.* **6**, Q3022 (2017).
- ¹¹M. J. Tadjer, N. A. Mahadik, V. D. Wheeler, E. R. Glaser, L. Ruppalt, A. D. Koehler, K. D. Hobart, C. R. Eddy, Jr., and F. J. Kub, *ECS J. Solid State Sci. Technol.* **5**, 468 (2016).
- ¹²M. Higashiwaki, K. Sasaki, T. Kamimura, M. H. Wong, D. Krishnamurthy, A. Kuramata, T. Masui, and S. Yamakoshi, *Appl. Phys. Lett.* **103**, 123511 (2013).
- ¹³M. Higashiwaki *et al.*, *Appl. Phys. Lett.* **108**, 133503 (2016).
- ¹⁴K. Konishi, K. Goto, H. Murakami, Y. Kumagai, A. Kuramata, S. Yamakoshi, and M. Higashiwaki, *Appl. Phys. Lett.* **110**, 103506 (2017).
- ¹⁵J. Kim, S. Oh, M. Mastro, and J. Kim, *Phys. Chem. Chem. Phys.* **18**, 15760 (2016).
- ¹⁶M. J. Tadjer, V. D. Wheeler, D. I. Shahin, C. R. Eddy, and F. J. Kub, *ECS J. Solid State Sci. Technol.* **6**, 165 (2017).
- ¹⁷K. Konishi, T. Kamimura, M. H. Wong, K. Sasaki, A. Kuramata, S. Yamakoshi, and M. Higashiwaki, *Phys. Status Solidi B* **253**, 623 (2016).
- ¹⁸T. Kamimura, K. Sasaki, M. H. Wong, D. Krishnamurthy, A. Kuramata, T. Masui, S. Yamakoshi, and M. Higashiwaki, *Appl. Phys. Lett.* **104**, 192104 (2014).
- ¹⁹V. D. Wheeler, D. I. Shahin, M. J. Tadjer, and C. R. Eddy, Jr., *ECS J. Solid State Sci. Technol.* **6**, Q3052 (2017).
- ²⁰J. Robertson and R. M. Wallace, *Mater. Sci. Eng., R* **88**, 1 (2015).
- ²¹D. C. Hays, B. P. Gila, and S. J. Pearton, *Appl. Phys. Rev.* **4**, 021301 (2017).
- ²²D. C. Hays, B. P. Gila, S. J. Pearton, A. Trucco, R. Thorpe, and F. Ren, *J. Vac. Sci. Technol., B* **35**, 011206 (2017).
- ²³D. C. Hays, B. P. Gila, S. J. Pearton, and F. Ren, *ECS J. Solid State Sci. Technol.* **5**, P680 (2016).
- ²⁴E. A. Kraut, R. W. Grant, J. R. Waldrop, and S. P. Kowalczyk, *Phys. Rev. Lett.* **44**, 1620 (1980).
- ²⁵E. A. Kraut, R. W. Grant, J. R. Waldrop, and S. P. Kowalczyk, *Phys. Rev. B* **28**, 1965 (1983).
- ²⁶E. Bersch, M. Di. S. Consiglio, R. D. Clark, G. J. Leusinkand, and A. C. Diebold, *J. Appl. Phys.* **107**, 043702 (2010).
- ²⁷H. C. Shin *et al.*, *Surf. Interface Anal.* **44**, 623 (2012).
- ²⁸Z. L. Wang and J. Bentley *Microsc. Res. Tech.* **20**, 390 (1992).
- ²⁹R. F. Egerton, *Electron Energy Loss Spectroscopy in the Electron Microscope* (Plenum, New York, 1996).
- ³⁰J. C. H. Spence, *Rep. Prog. Phys.* **69**, 725 (2006).
- ³¹S. Ren and M. Caricato, *J. Chem. Phys.* **144**, 184102 (2016).
- ³²P. H. Carey IV, F. Ren, D. C. Hays, B. P. Gila, S. J. Pearton, S. Jang, and A. Kuramata, *Vacuum* **141**, 103 (2017).
- ³³X. Guo, H. Zheng, S. W. King, V. V. Afanas'ev, M. R. Baklanov, J.-F. D. Marneffe, Y. Nishi, and J. L. Shohet, *Appl. Phys. Lett.* **107**, 082903 (2015).
- ³⁴J. Xu, Y. Teng, and F. Teng, *Sci. Rep.* **6**, 32457 (2016).
- ³⁵M. Yang, R. Q. Wu, Q. Chen, W. S. Deng, Y. P. Feng, J. W. Chai, J. S. Pan, and S. J. Wang, *Appl. Phys. Lett.* **94**, 142903 (2009).
- ³⁶A. Klein, *J. Phys.: Condens. Matter* **27**, 134201 (2015), available at <http://iopscience.iop.org/0953-8984/27/13/134201>.
- ³⁷F. Chen, R. Schafranek, S. Li, W. Wu, and A. J. Klein, *J. Phys. D* **43**, 295301 (2010).
- ³⁸T. Onuma, S. Fujioka, T. Yamaguchi, M. Higashiwaki, K. Sasaki, T. Matsui, and T. Honda, *Appl. Phys. Lett.* **103**, 041910 (2013).
- ³⁹H. He, R. Orlando, M. Blanco, and R. Pandey, *Phys. Rev. B* **74**, 195123 (2006).
- ⁴⁰J. B. Varley, J. R. Weber, A. Janotti, and C. G. Van de Walle, *Appl. Phys. Lett.* **97**, 142106 (2010).
- ⁴¹H. Peelaers and C. G. Van de Walle, *Phys. Status Solidi B* **252**, 828 (2015).
- ⁴²S. I. Stepanov, V. I. Nikolaev, V. E. Bougrov, and A. E. Romanov, *Rev. Adv. Mater. Sci.* **44**, 63 (2016), available at http://www.ipme.ru/e-journals/RAMS/no_14416/06_14416_stepanov.pdf.
- ⁴³Patrick H. Carey IV, F. Ren, David C. Hays, B. P. Gila, S. J. Pearton, Soohwan Jang, and Akito Kuramata, *Vacuum* **142**, 52 (2017).